

Theoretical Design of a Shallow Donor in Diamond by Lithium-Nitrogen Codoping

Jonathan E. Moussa,^{1,*} Noa Marom,¹ Na Sai,¹ and James R. Chelikowsky^{1,2}

¹*Center for Computational Materials, Institute of Computational Engineering and Sciences,
The University of Texas at Austin, Austin, Texas 78712*

²*Departments of Physics and Chemical Engineering,
The University of Texas at Austin, Austin, Texas 78712*

(Dated: July 21, 2018)

We propose a new substitutional impurity complex in diamond composed of a lithium atom that is tetrahedrally coordinated by four nitrogen atoms (LiN_4). Density functional calculations are consistent with the hydrogenic impurity model, both supporting the prediction that this complex is a shallow donor with an activation energy of 0.27 ± 0.06 eV. Three paths to the experimental realization of the LiN_4 complex in diamond are proposed and theoretically analyzed.

PACS numbers: 71.55.Cn, 71.15.Mb, 61.72.Bb

With respect to multiple figures of merit that estimate semiconductor performance in high-power electronics [1], diamond is the best of all known semiconductors. Steady progress is being made to realize diamond electronics by improving the quality and reducing the cost of single-crystal diamond films made by chemical vapor deposition (CVD) [2]. Substitutional boron doping has succeeded in producing p -type diamond and can be incorporated up to concentrations sufficient to cross the metal-insulator transition and produce superconductivity [3]. However, no donor impurity has been incorporated into single-crystal diamond with sufficiently small activation energy and high concentration to produce an n -type semiconductor suitable for high-power applications [4].

In this letter, we propose a new substitutional donor complex in diamond composed of lithium tetrahedrally coordinated by nitrogen and report on a theoretical study of its activation and formation. Favorable properties of LiN_4 can be inferred from properties of similar structures. Lithium tetraamine [5] is a metal composed of $\text{Li}(\text{NH}_3)_4$ molecules that are locally isostructural and isoelectronic to LiN_4 in diamond. Each $\text{Li}(\text{NH}_3)_4$ molecule donates an electron to a metallic state permeating the interstitial region between molecules. If this effect persists for dilute LiN_4 in diamond, it should produce shallow donor states with a small activation energy. A small formation energy is expected for LiN_4 based on the high stability of the B center in diamond [6], which is a vacancy (V) tetrahedrally coordinated by nitrogen, VN_4 .

Our proposal naturally follows from previous codoping proposals [7, 8] of multi-impurity complexes designed to prevent a carbon-nitrogen bond from breaking near a substitutional nitrogen impurity. The broken bond forms a deep, localized donor state. If the bond is preserved, the donor state is predicted to be shallower and more delocalized. The originally proposed BN_2 and newly proposed LiN_4 can be connected to nitrogen through a sequence of XN_n donor complexes, $\text{CN} \rightarrow \text{BN}_2 \rightarrow \text{BeN}_3 \rightarrow \text{LiN}_4$ (Fig. 1), by reducing the valence of the central atom and electronically compensating with neighboring nitrogens.

The study of other defects provides a useful reference, for comparison to XN_n and as a theoretical benchmark. We consider two well-known substitutional impurities, phosphorus and boron, and two artificial defects, C_5^{N} and C_5^{B} . C_5^{N} is a donor formed by adding an electron and compensating the charge by replacing a carbon and its four neighbors with fictional nuclei of nuclear charge $Z = 6.2$. C_5^{B} is a similarly constructed acceptor with $Z = 5.8$. This distribution of nuclear charge preserves the diamond lattice with minimal distortion and enables the formation of shallow defect levels.

The minimum activation energy of a point defect is estimated by the hydrogenic impurity model [9]. In this model, activation is independent of microscopic details of a defect. It depends only on bulk material properties: the dielectric constant ϵ and the ratio between a charge carrier's effective mass m^* [10] and the bare electron mass m . The defect loses a carrier to the nearby band edge, where it is Coulombically bound by $13.6 \frac{m^*}{m} \epsilon^{-2}$ eV to the ionized defect. This produces a donor level below the conduction band edge E_c or an acceptor level above the valence band edge E_v offset by the binding energy. Using experimental values [11], the model predicts defect levels at $E_c - 0.20$ eV and $E_v + 0.45$ eV in diamond compared to $E_c - 0.025$ eV and $E_v + 0.052$ eV in silicon.

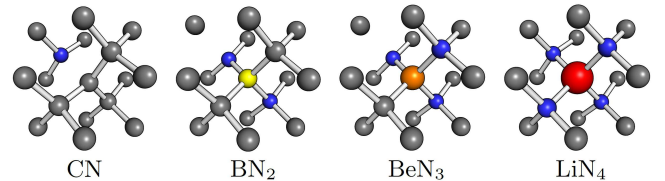


FIG. 1. (color online) Predicted structures of the XN_n donors. First and second neighbors from X are displayed. Bonds are omitted for unbonded carbon-nitrogen neighbors, all of which are separated by 2.0 Å. The remaining C-N bonds vary in length from 1.46 – 1.54 Å. The X -(C/N) bonds lengthen from right to left on the periodic table: 1.50 – 1.60 Å for B, 1.57 – 1.65 Å for Be, and 1.72 Å for Li.

Despite its simplicity, the hydrogenic impurity model is empirically successful. With acceptor levels measured at $E_v + 0.37$ eV in diamond and $E_v + 0.044$ eV in silicon, substitutional boron accurately fits the model. The substitutional phosphorus donor, at $E_c - 0.61$ eV in diamond [12] and $E_c - 0.045$ eV in silicon, is considered a shallow donor in silicon but not in diamond. Shallow donor levels at $E_c - 0.23$ eV have been reported in heavily deuterated samples of boron-doped diamond [13], but with a lifetime too short for applications.

A theoretical determination of whether LiN_4 is indeed a shallow donor requires treatment of microscopic details. We use a recently proposed method [14] that decomposes the donor activation energy Δ_D into a vertical ionization energy and structural relaxation energy,

$$\begin{aligned} \Delta_D &= E_c + E_{\text{tot}}^+(\mathbf{R}_D^+) - E_{\text{tot}}^0(\mathbf{R}_D^0) \\ &= \underbrace{[E_c - E_D(\mathbf{R}_D^+)]}_{\Delta_D^{\text{ionize}}} + \underbrace{[E_{\text{tot}}^0(\mathbf{R}_D^+) - E_{\text{tot}}^0(\mathbf{R}_D^0)]}_{\Delta_D^{\text{relax}}}. \end{aligned} \quad (1)$$

$E_{\text{tot}}^Q(\mathbf{R})$ is the total energy of the system with net charge Q and atomic coordinates \mathbf{R} . $E_D(\mathbf{R})$ is the donor energy level, equal to $E_{\text{tot}}^0(\mathbf{R}) - E_{\text{tot}}^+(\mathbf{R})$. The equilibrium atomic coordinates of the donor-containing structure with net charge Q is denoted by \mathbf{R}_D^Q . The corresponding expression for an acceptor activation energy Δ_A is

$$\Delta_A = \underbrace{[E_A(\mathbf{R}_A^-) - E_v]}_{\Delta_A^{\text{ionize}}} + \underbrace{[E_{\text{tot}}^0(\mathbf{R}_A^-) - E_{\text{tot}}^0(\mathbf{R}_A^0)]}_{\Delta_A^{\text{relax}}}. \quad (2)$$

This decomposition into elementary excitation processes is not unique [15], but it enables separate calculations of Δ^{relax} with total energy methods and Δ^{ionize} with more sophisticated and accurate quasiparticle methods.

Total energies and equilibrium crystal structures are calculated with density functional theory (DFT) [16, 17] using the Perdew-Burke-Ernzerhof (PBE) functional [18]. C_5^{B} and C_5^{N} are modeled with alchemical pseudopotentials [19]. Isolated defects are approximated with a periodic array of defects in a supercell of diamond. We use a $6 \times 6 \times 6$ face-centered cubic supercell (432 carbon atoms when defect-free), consistent with previous studies [20]. Supercells with nonzero net charge are simulated with a neutralizing jellium charge distribution.

All defect structures are relaxed in their neutral and ionized states from multiple random perturbations of the ideal diamond lattice. Stable neutral XN_n structures are shown in Fig. 1. BN_2 and BeN_3 also have metastable structures. Metastable BN_2 is similar to its originally predicted structure [7], with two elongated C-N bonds of length 1.80 Å rather than a single fully broken C-N bond. The remaining structures, including metastable BeN_3 and all ionized defects, produce minor distortions in the diamond lattice that are well approximated by one bond length for each bonded pair of elements.

Quasiparticle methods, unlike DFT, are constructed to directly model charge excitation energies such as Δ^{ionize} . The state-of-the-art is the *GW* method [21], which is too expensive to apply to large supercells at present. Instead, we use the recently proposed “PBE- ϵ ” method [22], which approximates the quasiparticle self-energy as

$$\begin{aligned} \Sigma_{\text{PBE-}\epsilon}(\mathbf{r}, \mathbf{r}') &= [(1 - \epsilon^{-1})v_x^{\text{PBE}}(\mathbf{r}) + v_c^{\text{PBE}}(\mathbf{r})] \delta(\mathbf{r} - \mathbf{r}') \\ &\quad - \epsilon^{-1} \rho(\mathbf{r}, \mathbf{r}') V(\mathbf{r} - \mathbf{r}'), \end{aligned} \quad (3)$$

with the PBE exchange $v_x^{\text{PBE}}(\mathbf{r})$ and correlation $v_c^{\text{PBE}}(\mathbf{r})$ potentials and a screened Fock exchange composed of the 1-particle density matrix $\rho(\mathbf{r}, \mathbf{r}')$ and the Coulomb kernel, $V(\mathbf{r} - \mathbf{r}') = e^2/|\mathbf{r} - \mathbf{r}'|$. With the dielectric constant ϵ set to the experimental value [11], this method produces a 5.48 eV band gap for diamond, comparing well to the experimental value of 5.5 eV.

PBE- ϵ is an adequate quasiparticle method for shallow impurity calculations because it approximates the basic physics of a charge carrier bound to an ionized defect. As in the hydrogenic impurity model, a donor state $\psi_D(\mathbf{r})$ should see an effective Hartree potential originating from a screened ionized donor of net charge ϵ^{-1} . Upon adding a neutral donor to pristine diamond, the Hartree potential is modified by contributions from an updated nuclear charge, $\delta\rho_{\text{ion}}(\mathbf{r})$, and an added donor electron charge,

$$\delta v_H(\mathbf{r}) = \int V(\mathbf{r} - \mathbf{r}') [|\psi_D(\mathbf{r}')|^2 - \delta\rho_{\text{ion}}(\mathbf{r}')] d\mathbf{r}'. \quad (4)$$

The donor state also sees a modified effective potential from its self interaction in the screened Fock exchange,

$$- \int \epsilon^{-1} \psi_D(\mathbf{r}) \psi_D^*(\mathbf{r}') V(\mathbf{r} - \mathbf{r}') \psi_D(\mathbf{r}') d\mathbf{r}' = \delta v_{sX}(\mathbf{r}) \psi_D(\mathbf{r})$$

$$\delta v_{sX}(\mathbf{r}) = -\epsilon^{-1} \int V(\mathbf{r} - \mathbf{r}') |\psi_D(\mathbf{r}')|^2 d\mathbf{r}'. \quad (5)$$

The total donor-induced potential is $\delta v_H(\mathbf{r}) + \delta v_{sX}(\mathbf{r})$, which corresponds to the bare ionized donor $\delta\rho_{\text{ion}}(\mathbf{r})$ and an effective screening cloud $(\epsilon^{-1} - 1)|\psi_D(\mathbf{r})|^2$. A similar argument applies to acceptors. The screening cloud has the right net charge but the wrong length scale: the Bohr radius of the donor state is 6.3 Å, but the screening length in diamond is estimated to be 1.5 Å [23]. We find PBE- ϵ to be a good compromise between costly *GW* corrections to the screening length and PBE without Fock exchange, which has an effective screening cloud of unit charge that suppresses the long-range electron-impurity interaction and produces a donor impurity band nearly degenerate with the conduction band edge [17].

The periodic array of defects broadens defect levels into bands up to 0.4 eV in width. Modeling or extrapolation is necessary to extract an accurate activation energy. We use a tight-binding ansatz and a range of supercells from $5 \times 5 \times 5$ to $8 \times 8 \times 8$ for extrapolation, which is described in detail in the Supplemental Material [17].

TABLE I. Donor and acceptor activation energies calculated with both the marker method [20] and PBE- ϵ quasiparticles, compared to experiment. PBE- ϵ results are separated into relaxation and ionization contributions, $\Delta^{\text{PBE-}\epsilon} = \Delta^{\text{ionize}} + \Delta^{\text{relax}}$, as in Eqs. (1) and (2). $\delta\Delta^{\text{ionize}}$ is the RMS variance of extrapolation [17]. All energies are in units of eV.

Defect	Δ^{exp}	Δ^{marker}	$\Delta^{\text{PBE-}\epsilon}$	Δ^{ionize}	$\delta\Delta^{\text{ionize}}$	Δ^{relax}
C_5^{N}	...	0.45	0.31	0.31	0.03	0.00
LiN_4	...	0.48	0.27	0.27	0.03	0.00
BeN_3^{a}	...	0.56	0.40	0.39	0.04	0.01
P	0.61	0.61 ^b	0.56	0.54	0.02	0.02
BeN_3	...	0.78	0.62	0.39	0.04	0.23
BN_2^{a}	...	0.88	0.77	0.50	0.03	0.27
BN_2	...	1.30	1.19	0.50	0.03	0.69
N	1.7	1.67	1.71	0.86	0.04	0.85
C_5^{B}	...	0.31	0.30	0.30	0.01	0.00
B	0.37	0.37 ^b	0.31	0.31	0.03	0.00

^a Metastable structure.

^b Experimental marker.

Theoretical activation energies are listed in Table I alongside known experimental values. The PBE- ϵ quasiparticle approach is compared to the semi-empirical marker method [20], which calculates activation energies relative to an experimental “marker” impurity using PBE total energy differences. The marker method predicts larger activation energies than PBE- ϵ . These deviations grow with decreasing activation energy and become as large as the value we are attempting to predict. This can be explained by delocalization errors in PBE that are reduced in PBE- ϵ with the addition of Fock exchange [15]. Therefore, PBE- ϵ should be more reliable than the marker method as a predictor of activation energies over a wider energy range. Doubling the extrapolation variance provides a wide enough confidence interval for the PBE- ϵ predictions to be consistent with all experiments. LiN_4 is shallower than the artificial shallow donor C_5^{N} and an activation energy of 0.27 ± 0.06 eV is consistent with the hydrogenic impurity model. We conclude that LiN_4 is a shallow donor.

Having confirmed the viability of LiN_4 as a shallow donor in diamond, we now consider three synthesis paths. The first path is the diffusion of lithium into diamond [24] with a high concentration of B centers (VN_4). The second path is high-pressure, high-temperature (HPHT) diamond synthesis [25] in the presence of lithium and nitrogen. The third path is CVD diamond synthesis with the LiN_4 impurity preformed in a seed material [26] or deposited molecule [27].

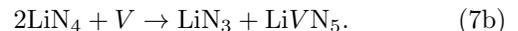
Nitrogen incorporates substitutionally into diamond, found as an isolated center, a dimer, or clustered around a vacancy, VN_m [6]. High temperature treatment causes vacancies to become mobile and cluster with nitrogen to

form mobile VN_m complexes. Theoretical studies of Li diffusion in N-free diamond [28] predict the interstitial (Li_i) to be a mobile donor that is strongly trapped by vacancies. The natural extension to N-rich diamond is a general trapping process, $\text{Li}_i + \text{VN}_m \rightarrow \text{LiN}_m$, which we calculate to bind at 6.88, 7.24, 8.04, 8.37, and 6.08 eV for $m = 0, \dots, 4$. All sites trap strongly, but VN_4 is preferred least by Li_i . The LiN_m defect sequence has a regular trend of activity from triple acceptor ($m = 0$) to single donor ($m = 4$). Assuming all vacancies will be filled with lithium and the only acceptors are Li, LiN, and LiN_2 , then the defect concentrations $n(X)$ must satisfy the inequality

$$n(\text{LiN}_4) > 3n(\text{Li}) + 2n(\text{LiN}) + n(\text{LiN}_2) \quad (6)$$

to prevent all LiN_4 from being passivated. Therefore, lithium diffusion into a diamond sample is only likely to succeed in producing active LiN_4 if the average number of nitrogens around each vacancy in the pre-lithiated sample is greater than 3.

HPHT synthesis of LiN_4 at a detectable concentration requires sufficient thermodynamic stability of the complex at an accessible pressure and temperature. At zero temperature, we have found two pairwise decomposition processes that passivate shallow donor activity,



The first reaction produces a LiN_4 dimer with neighboring nitrogens that break the N-N bond, which only lowers enthalpy below 530 GPa. The second reaction exchanges a nitrogen and binds an additional vacancy to the N-rich complex, which produces an octahedrally coordinated Li surrounded by CN_5 . Assuming a zero chemical potential for V , this process lowers enthalpy at all tested pressures (up to 700 GPa) and has a minimum enthalpy reduction of 2.47 eV at 210 GPa. As a result of the process in Eq. (7b), it is unlikely that LiN_4 can be synthesized in HPHT or any other conditions that enable LiN_4 and V to become mobile and interact with each other.

Formation of the LiN_4 complex in a CVD process from separate lithium and nitrogen sources is likely to be a rare event because it involves a coincidence of five atoms, each with a presumably low concentration. This problem can be avoided by preforming the complex within a precursor molecule. A suitable LiN_4 precursor should be small to enhance volatility and simplify synthesis, closely conform to the diamond lattice it is to be incorporated into, and exist as a well-defined lithium-free molecule that strongly binds a lithium atom or ion. Diamondoids [29] satisfy the second constraint and many chelants [30] satisfy the third constraint, but we propose a new analog of cyclododecane (Fig. 2) that satisfies all three constraints (with IUPAC name 1,7-diazacyclododecane-4,10-diamine). Lithiation

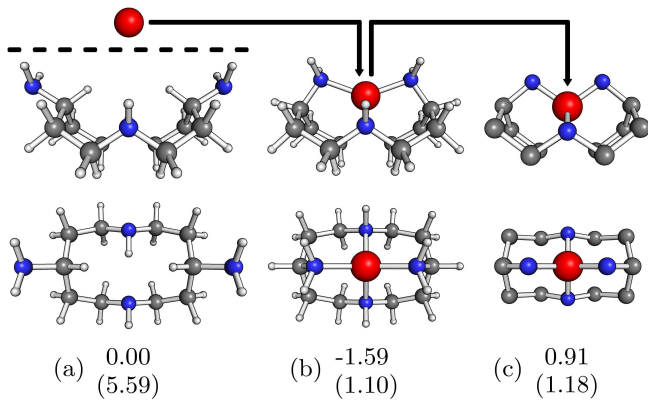


FIG. 2. (color online) Top and side views of (a) isolated Li and 1,7-diazacyclododecane-4,10-diamine, (b) Li bound to 1,7-diazacyclododecane-4,10-diamine, and (c) Li bound to the VN_4 defect in diamond. Relative formation energies of Li (and Li^+ in parentheses) are reported in eV, from PBE total energies (and PBE- ϵ ionization energy for Li^+ in (c)). The structures for Li^+ are similar to the neutral structures shown.

of this molecule should abstract H (as $\frac{1}{2}H_2$) to form a more stable (by 0.24 eV in our calculations) lithamide.

Figure 2 depicts lithium in three metastable positions relevant to CVD: the isolated atom, bound to a precursor molecule, and bound to a B center in diamond. Li^+ is strongly bound to both sites. Li is not bound to the B center, but will remain trapped there because of a large energy barrier. The Li-N bond length of 2.0 Å within the precursor is reduced to 1.72 Å within the B center. Bond strain can be quantified indirectly by comparing total energies of the relaxed VN_4 cavity to the LiN_4 defect structure with Li removed, which results in a difference of 0.27 eV. The reduction of LiN_4 's ionization energy from the precursor to diamond is caused by a destabilization of the neutral state rather than any significant change of the ionized state.

Successful CVD synthesis of LiN_4 is contingent on the existence of growth conditions that preserve the internal structure of the LiN_4 precursor while still enabling good diamond crystal formation, which is an open problem.

In short, we propose LiN_4 as a new donor complex in diamond with a predicted activation energy of 0.27 ± 0.06 eV. Synthesis of LiN_4 is likely to require that Li be reacted with a preformed VN_4 complex, either within diamond or a precursor molecule. While further studies of Li-N-V defect chemistry in diamond are warranted, the present result should serve as sufficient impetus for the pursuit of experimental realization of LiN_4 .

We acknowledge support from the National Science Foundation under Grant No. DMR-0941645. Computing resources were provided by the National Energy Research Scientific Computing Center (NERSC). Alchemical pseudopotentials and VASP modifications required for their use were kindly provided by Daniel Sheppard. Molecular

visualizations were generated with PYMOL [31]. J.E.M. thanks Jay Deep Sau for helpful discussions.

* godotalgorithm@gmail.com

- [1] B. J. Baliga, IEEE Electron Device Lett., **10**, 455 (1989).
- [2] P. W. May, Science, **319**, 1490 (2008).
- [3] T. Klein *et al.*, Phys. Rev. B, **75**, 165313 (2007).
- [4] R. Kalish, J. Phys. D, **40**, 6467 (2007).
- [5] E. Zurek, X.-D. Wen, and R. Hoffmann, J. Am. Chem. Soc., **133**, 3535 (2011).
- [6] T. Evans, in *The Properties of Natural and Synthetic Diamond*, edited by J. E. Field (Academic Press, 1992) Chap. 6, pp. 259–290.
- [7] H. Katayama-Yoshida, T. Nishimatsu, T. Yamamoto, and N. Orita, Phys. Status Solidi B, **210**, 429 (1998).
- [8] D. Segev and S.-H. Wei, Phys. Rev. Lett., **91**, 126406 (2003).
- [9] S. T. Pantelides, Rev. Mod. Phys., **50**, 797 (1978).
- [10] For electrons, m_e^* is averaged assuming an anisotropic conduction band as $(m_e^*)^{-1} = [(m_{e\parallel}^*)^{-1} + 2(m_{e\perp}^*)^{-1}]/3$. For holes, m_h^* is taken from the heavy hole band.
- [11] O. Madelung, *Semiconductors: Data Handbook*, 3rd ed. (Springer-Verlag, Berlin, 2004) Unless otherwise noted, all quoted experimental values are from this reference. For diamond: $\epsilon = 5.7$, $m_e^* = 0.48 m$, $m_h^* = 1.08 m$. For silicon: $\epsilon = 11.9$, $m_e^* = 0.26 m$, $m_h^* = 0.54 m$.
- [12] E. Gheeraert, S. Koizumi, T. Teraji, and H. Kanda, Solid State Commun., **113**, 577 (2000).
- [13] Z. Teukam *et al.*, Nature Mater., **2**, 482 (2003).
- [14] M. Hedström *et al.*, Phys. Rev. Lett., **97**, 226401 (2006).
- [15] N. Sai, P. F. Barbara, and K. Leung, Phys. Rev. Lett., **106**, 226403 (2011).
- [16] G. Kresse and J. Hafner, Phys. Rev. B, **47**, 558 (1993); **49**, 14251 (1994); G. Kresse and J. Furthmüller, Comput. Mater. Sci., **6**, 15 (1996); Phys. Rev. B, **54**, 11169 (1996).
- [17] See Supplemental Material for computational details.
- [18] J. P. Perdew, K. Burke, and M. Ernzerhof, Phys. Rev. Lett., **77**, 3865 (1996).
- [19] D. Sheppard, G. Henkelman, and O. A. von Lilienfeld, J. Chem. Phys., **133**, 084104 (2010).
- [20] J. P. Goss, P. R. Briddon, and R. J. Eyre, Phys. Rev. B, **74**, 245217 (2006).
- [21] G. Onida, L. Reining, and A. Rubio, Rev. Mod. Phys., **74**, 601 (2002).
- [22] M. A. L. Marques *et al.*, Phys. Rev. B, **83**, 035119 (2011).
- [23] R. Resta, Phys. Rev. B, **16**, 2717 (1977).
- [24] C. Uzan-Saguy *et al.*, Phys. Status Solidi A, **193**, 508 (2002).
- [25] E. A. Ekimov *et al.*, Nature (London), **428**, 542 (2004).
- [26] K. Tsugawa *et al.*, J. Phys. Chem. C, **114**, 3822 (2010).
- [27] H. Sternschulte, M. Schreck, B. Stritzker, A. Bergmaier, and G. Dollinger, Diam. Relat. Mater., **9**, 1046 (2000).
- [28] J. P. Goss and P. R. Briddon, Phys. Rev. B, **75**, 075202 (2007).
- [29] J. E. Dahl, S. G. Liu, and R. M. K. Carlson, Science, **299**, 96 (2003).
- [30] M. Formica *et al.*, Coord. Chem. Rev., **184**, 347 (1999).
- [31] “PYMOL Molecular Visualization System,” version 1.2r1, <http://www.pymol.org/>.

Supplemental Material to “Theoretical Design of a Shallow Donor in Diamond by Lithium-Nitrogen Codoping”

All DFT calculations are performed using version 5.2 of the Vienna Ab-initio Simulation Package (VASP) [1]. A planewave cutoff of 400 eV is used for all calculations, along with the manual-recommended [2] projector augmented-wave pseudopotentials (or alchemical mixtures thereof [3]). Band occupations are set by Gaussian smearing with a width of 0.01 eV. Relaxed structures have the forces on all atoms reduced below 0.1 eV/Å. The PBE lattice constant of 3.57 Å is used for all calculations in diamond at zero pressure. Finite pressure is simulated by reducing the lattice constant. A $2 \times 2 \times 2$ Monkhorst-Pack grid is used to sample the Brillouin zone (BZ) of diamond supercells for PBE total energy calculations, as suggested in previous studies [4]. All molecules are simulated at the Γ -point of a cubic supercell with a 20 Å lattice constant. Predictions of molecular structure are made by generating many locally stable conformations using the MMFF94s force field in AVOGADRO [5] and further relaxing them in VASP. The lowest energy structure found by this search is presumed to be the ground state.

The computational cost of PBE- ϵ calculations is larger than PBE because of the Fock exchange step. The ratio between costs grows linearly with the number of points used to sample the BZ, which limits our PBE- ϵ calculations to a single BZ point at a time for large supercells. When computing the band structure at a BZ point, the density matrix is constructed from only that BZ point and iterated to self-consistency. This is a systematic error for finite supercells, but it is exponentially suppressed with increasing supercell size because all bands are fully occupied (half-filled impurity bands are fully occupied in one spin channel and empty in the other).

The addition of Fock exchange in switching from PBE to PBE- ϵ has the basic effect of making the impurity bands deeper and more sensitive to finite-size effects. This is illustrated in Fig. 3 with a plot of the lowest branch of the conduction band and the donor impurity band of LiN_4 in a $6 \times 6 \times 6$ supercell along the $L - \Gamma - X$ high symmetry path. PBE and PBE- ϵ produce similar results, except that the PBE- ϵ impurity band is rigidly shifted downwards in energy by 0.68 eV. The average depth of the PBE impurity band is smaller than the expected shallow impurity depth of 0.2 eV and does not change significantly in larger supercells. The PBE- ϵ impurity band is deeper than expected, but it becomes more shallow with increasing supercell size and decreasing impurity density. To estimate the isolated impurity limit, some kind of extrapolation must be performed.

We calculate impurity ionization energies Δ^{ionize} by using a range of diamond supercells from $5 \times 5 \times 5$ to $8 \times 8 \times 8$. Smaller supercells have finite-size effects that are too large and complicated to be fit to a simple extrapolation model and larger supercells are computationally

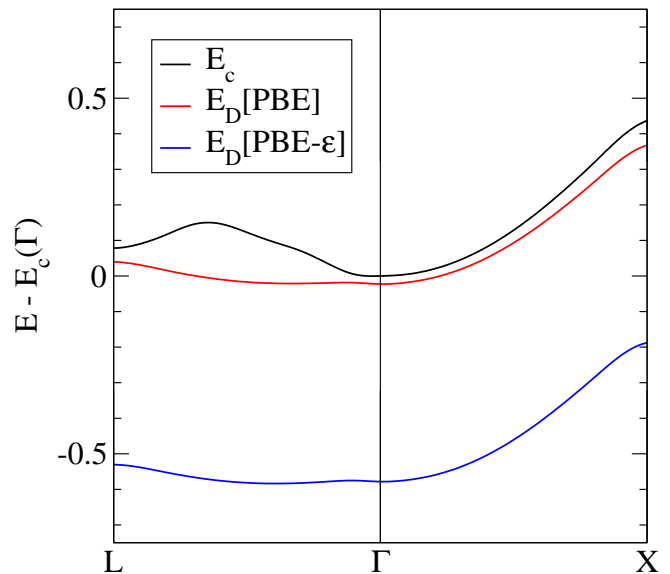


FIG. 3. PBE and PBE- ϵ band structures of LiN_4 in a $6 \times 6 \times 6$ supercell in the spin channel where the donor impurity band is occupied. Only the donor impurity band and the lowest branch of the conduction band are shown. The conduction band is similar at both levels of theory and only one is plotted.

intractable. We assume a tight binding picture where impurity states are localized about each impurity and an impurity band manifests from hopping between impurity states. The hopping energy and impurity bandwidth should decrease exponentially with increasing distance between neighboring impurities R . All finite-size effects in the impurity band should follow a simple exponential form $\propto \exp(-R/R_0)$. R_0 is an estimate of the effective Bohr radius of the impurity state, but it may be partially contaminated by finite-size BZ sampling errors. If the finite-size dependence is similar and simple enough, then some combination of BZ points in the impurity band should cancel the finite-size effects. Specifically, we make a simple but arbitrary choice to define

$$\Delta_D^{\text{ionize}} \approx E_c(\Gamma) - [(1-x)E_D(\Gamma) + xE_D(X)] \quad (8a)$$

$$\Delta_A^{\text{ionize}} \approx [(1-x)E_A(\Gamma) + xE_A(X)] - E_v(\Gamma), \quad (8b)$$

where E_c is the lowest branch of the conduction band, E_v is the highest branch of the valence band, E_D is the occupied donor impurity band, and E_A is the unoccupied acceptor impurity band. For large supercells, this expression will be independent of the choice of x . With this free parameter and the results from 4 supercells, we perform a least squares fit to minimize the size-dependence of Δ^{ionize} in Eq. (8) about an asymptotic ionization energy. Additionally, we fit $E_D(X) - E_D(\Gamma)$ and $E_A(\Gamma) - E_A(X)$ to the form $C \exp(-R/R_0)$ to estimate R_0 .

Extrapolation results are tabulated in Table II. $\delta\Delta^{\text{ionize}}$ is the root-mean-square (RMS) deviation between the extrapolated Δ^{ionize} and Eq. (8) for the 4

TABLE II. Extrapolated donor and acceptor properties. R_0 is the effective Bohr radius in Å. Δ^{ionize} is the ionization energy and $\delta\Delta^{\text{ionize}}$ is its RMS variance, both in eV. x is the parameter used in the extrapolation formulae in Eq. (8).

Defect	R_0	Δ^{ionize}	$\delta\Delta^{\text{ionize}}$	x
C_5^{N}	7.9	0.31	0.03	0.74
LiN_4	7.8	0.27	0.03	0.74
BeN_3	6.7	0.39	0.04	0.69
BN_2	5.5	0.50	0.03	0.62
P	5.2	0.54	0.02	0.61
N	4.5	0.86	0.04	1.04
B	7.9	0.31	0.03	1.05
C_5^{B}	7.0	0.30	0.01	0.95

calculated supercells. The extrapolation procedure succeeds in reducing the variance to a value significantly below the bandwidth of the impurity bands in the calculated supercells. The effective Bohr radii extracted from extrapolation increase with decreasing ionization energy,

as expected from a simple hydrogenic model of impurities. The hydrogenic impurity model gives a radius of 6.3 Å for shallow donors and 2.8 Å for shallow acceptors, which is smaller than the extrapolated values and especially so for the acceptors. The cause of this deviation is unclear, but the effect on the ionization energies seems minor since boron is within 0.06 eV of its experimental activation energy of 0.37 eV.

* godotalgorithm@gmail.com

- [1] G. Kresse and J. Hafner, Phys. Rev. B, **47**, 558 (1993); **49**, 14251 (1994); G. Kresse and J. Furthmüller, Comput. Mater. Sci., **6**, 15 (1996); Phys. Rev. B, **54**, 11169 (1996).
- [2] <http://cms.mpi.univie.ac.at/vasp/vasp/vasp.html>.
- [3] D. Sheppard, G. Henkelman, and O. A. von Lilienfeld, J. Chem. Phys., **133**, 084104 (2010).
- [4] J. P. Goss, P. R. Briddon, and R. J. Eyre, Phys. Rev. B, **74**, 245217 (2006).
- [5] <http://avogadro.openmolecules.net>.